Mechanics of Advanced Composite Structures 4 (2017) 75-87

Semnan University

Mechanics of Advanced Composite Structures

journal homepage: http://MACS.journals.semnan.ac.ir

A Numerical and Analytical Solution for the Free Vibration of Laminated Composites Using Different Plate Theories

M.A. Torabizadeh [a*], A. Fereidoon [b]

[a] *Department of Mechanical Engineering, University of Applied Science and Technology, Mashhad, Iran*
[b] *Department of Mechanical Engineering, University of Semnan, Semnan, Iran*

PAPER INFO

Paper history:
Received 2016-11-27
Revised 2017-01-21
Accepted 2017-02-09

Keywords:
Free vibration
Laminated composites
Plate theories
Numerical method
Analytical method

ABSTRACT

An analytical and numerical solution for the free vibration of laminated polymeric composite plates with different layups is studied in this paper. The governing equations of the laminated composite plates are derived from the classical laminated plate theory (CLPT) and the first-order shear deformation plate theory (FSDT). General layups are evaluated by the assumption of cross-ply and angle-ply laminated plates. The solver is coded in MATLAB. As a verification method, a finite element code using ANSYS is also developed. The effects of lamination angle, plate aspect ratio and modulus ratio on the fundamental natural frequencies of a laminated composite are also investigated and good agreement is found between the results evaluated and those available in the open literature. The results show that the fundamental frequency increases with the modular ratio and the bending-stretching coupling lowers the vibration frequencies for both cross-ply and angle-ply laminates with the CLPT. Also it is found that the effect of bending-stretching coupling, transverse shear deformation and rotary inertia is to lower the fundamental frequencies.

DOI: 10.22075/MACS.2017.1768.1090

1. Introduction

A composite material can be defined as a combination of two or more materials that results in better properties than those of the individual components used alone. In contrast to metallic alloys, each material retains its separate chemical, physical and mechanical properties. The two constituents are reinforcement and a matrix. When composites are compared to bulk materials, the main advantages of composite materials are their high strength and stiffness, combined with low density, allowing for a weight reduction in the finished part. The reinforcing phase provides the strength and stiffness. In most cases, the reinforcement is harder, stronger and stiffer than the matrix. The reinforcement is usually a fiber or a particulate. Particulate composites have dimensions that are approximately equal in all directions. They may be spherical, platelets, or any other regular or irregular geometry. Particulate composites tend to be much weaker and less stiff than continuous-fiber composites, but they are usually much less expensive. Particulate reinforced composites usually contain less reinforcement (up to 40 volume percent to 50 volume percent) due to processing difficulties and brittleness [1].

A fiber's length is much greater than its diameter. The length-to-diameter (l/d) ratio is known as the aspect ratio and can vary greatly. Continuous fibers have long aspect ratios, whereas discontinuous fibers have short ones. Continuous-fiber composites normally have a preferred orientation, whereas discontinuous fibers generally have a random orientation. Examples of continuous reinforcements include unidirectional, woven cloth and helical winding, whereas examples of discontinuous reinforcements are chopped fibers and random material. Continuous-fiber composites are often made into laminates by stacking single sheets of continuous fibers in different orientations to obtain the desired

* Corresponding author. Tel.: +98-51-38552304; Fax: +98-51-38531907

E-mail address: m.torabizadeh@uast.ac.ir

strength and stiffness properties with fiber volumes as high as 60 percent to 70 percent. Fibers produce high-strength composites because of their small diameter; they contain far fewer defects (normally surface defects) compared to those in the material produced in bulk. As a general rule, the smaller the diameter of the fiber, the higher its strength, but often the cost increases as the diameter becomes smaller. In addition, smaller-diameter/high-strength fibers have greater flexibility and are more amenable to fabrication processes, such as weaving or forming over radius. Typical fibers include glass, aramid and carbon, which may be continuous or discontinuous. The continuous phase is the matrix, which is a polymer, metal or ceramic. Polymers have low strength and stiffness, metals have intermediate strength and stiffness but high ductility, and ceramics have high strength and stiffness but are brittle. The matrix (continuous phase) performs several critical functions, including maintaining the fibers in the proper orientation and spacing and protecting them from abrasion and the environment. In polymer and metal matrix composites that form a strong bond between the fiber and the matrix, the matrix transmits loads from the matrix to the fibers through shear loading at the interface. In ceramics-matrix composites, the objective is often to increase the toughness rather than the strength and stiffness; therefore, a low interfacial strength bond is desirable [1].

Tan and Nie [2] studied free and forced vibration of variable stiffness composite annular thin plates with elastically restrained edges based on the classical plate theory. They found that the transverse mode shapes of the plates with in-plane variable stiffness are different from those with constant stiffness. Zhang et al. [3] analyzed free vibration analysis of triangular CNT-reinforced composite plates subjected to in-plane stresses using the FSDT element-free method. Chakraborty et al. [4] presented a novel approach, referred to as polynomial correlated function expansion (PCFE), for a stochastic free-vibration analysis of a composite laminate. Finally, based on the numerical results, new physical insights had been created on the dynamic behavior of composite laminates. Ganesh et al. [5] studied the free vibration analysis of delaminated composite plates using a finite element method. Mantari and Ore [6] presented a simplified first-order shear deformation theory (FSDT) for a laminated composite and sandwich plates. Their approach had a novel displacement field that includes undetermined integral terms and contains only four unknowns. Su et al. [7] illustrated a modified Fourier series to study the free vibration of a laminated composite and four-parameter functionally graded sector plates with general boundary conditions. Zhang et al. [8] studied the free-vibration analysis of functionally graded carbon nanotube-reinforced composite triangular plates using the FSDT and the element-free IMLS-Ritz method. They also examined the influence of a carbon nanotube volume fraction, plate thickness-to-width ratio, plate-aspect ratio and a boundary condition on the plate's vibration behavior. Marjanović and Vuksanović [9] illustrated a layerwise solution to free vibrations and the buckling of a laminated composite and sandwich plates with embedded delamination. The effects of plate geometry, lamination scheme, degree of orthotropy and delamination size or position on the dynamic characteristics of the plate were presented. Boscolo [10] presented an analytical closed-form solution for a free-vibration analysis of multilayered plates by using a layer-wise displacement assumption based on Carrera's Unified Formulation. A wide range of boundary conditions were analyzed by using a Levy-type solution. Ou et al. [11] presented an efficient method for predicting the free and transient vibrations of multilayered composite structures with parallelepiped shapes, including beams, plates and solids. Rafiee et al. [12] analyzed the geometrically nonlinear free vibration of shear deformable piezoelectric carbon nanotube/fiber/polymer multiscale laminated composite plates. Akhras and Li [13] used a spline finite strip with higher-order shear deformation for stability and a free-vibration analysis of piezoelectric composite plates. Grover et al. [14] assessed a new shear deformation theory for free-vibration-response laminated composite and sandwich plates. They compared the results with finite element and analytical solutions. Jafari et al. [15] presented a free-vibration analysis of a generally laminated composite beam (LCB) based on the Timoshenko beam theory using the method of Lagrange multipliers. They examined some parameters, such as the slenderness ratio, the rotary inertia, the shear deformation, material anisotropy, ply configuration and boundary conditions on the natural frequency and mode shape. Tai and Kim [16] illustrated the free vibration of laminated composite plates using two variable refined plate theories. They applied the Navier technique to obtain the closed-form solutions of antisymmetric cross-ply and angle-ply laminates. Srinivasa et al. [17] and Ramu and Mohanty [18] used finite element results as a verification method with those obtained from experimental tests on the free vibration of composite plates. Chandrashekhara [19] presented an exact solution for the free vibration of symmetrically laminated composite beams. Ke et al. [20] investigated the nonlinear free vibration of functionally graded nanocomposite beams reinforced by single-walled carbon nanotubes (SWCNTs) based on the Timoshenko beam theory and von Kármán geometric nonlinearity. Also, the free vibration of anisotropic thin-walled composite beams and delaminated composite beams were performed by Song [21] and Lee [22], respectively.

Based on papers reviewed in the literature, few investigations were found that compared the analytical and numerical analyses of different theories and lamination layups. Therefore, in this paper, the analytical

and numerical solutions for the free vibration of laminated polymeric composite plates with different layups are compared. Two different theories and layups are selected. Also, finite-element analysis is performed using ANSYS to validate results obtained by analytical methods. The solver is coded in MATLAB. Also investigated are the effects of different parameters, such as the lamination angle, the plate aspect ratio and the modulus ratio on the fundamental natural frequencies of laminated composite. The main objective of this paper is to compare different theories and lamination schemes on the vibration response of laminated composites.

2. Theoretical Formulation

2.1. Classical lamination plate theory (CLPT)

2.1.1 Displacement and strains

A rectangular plate of sides a and b with thickness h is shown in Fig. 1. Based on the classical lamination plate theory, the following displacement field can be assumed [23]:

$$u(x,y,z,t) = u_0(x,y,t) - z\frac{\partial w_0}{\partial x} \tag{1}$$

$$v(x,y,z,t) = v_0(x,y,t) - z\frac{\partial w_0}{\partial y} \tag{2}$$

$$w(x,y,z,t) = w_0(x,y,t) \tag{3}$$

where u_0, v_0, w_0 are the displacements along the coordinate lines of a material point on xy-plane.

The von Karman strains associated with the displacement field in static loading can be computed using the strain-displacement relations for small strains:

$$\varepsilon_{xx} = \frac{\partial u_0}{\partial x} - z\frac{\partial^2 w_0}{\partial x^2}, \varepsilon_{xz} = \varepsilon_{yz} = \varepsilon_{xz} = 0$$
$$\varepsilon_{yy} = \frac{\partial v_0}{\partial y} - z\frac{\partial^2 w_0}{\partial y^2} \tag{4}$$
$$\varepsilon_{xy} = \frac{1}{2}\left(\frac{\partial u_0}{\partial y} + \frac{\partial v_0}{\partial x}\right) - z\frac{\partial^2 w_0}{\partial x \partial y}$$

Note that the transverse strains are identically zero in classical plate theory. The first three strains have the form

$$\begin{Bmatrix}\varepsilon_{xx}\\ \varepsilon_{yy}\\ \varepsilon_{xy}\end{Bmatrix} = \begin{Bmatrix}\varepsilon^0_{xx}\\ \varepsilon^0_{yy}\\ \varepsilon^0_{xy}\end{Bmatrix} + z\begin{Bmatrix}\varepsilon^1_{xx}\\ \varepsilon^1_{yy}\\ \varepsilon^1_{xy}\end{Bmatrix} \tag{5}$$

2.1.2 Equilibrium equations

By using Eqs. (4) and (5), the constitutive equations are obtained. Equations of equilibrium can be derived using the variational principle, which is not explained in detail here (see [23]). The Euler-Lagrange equations of the theory are obtained as follows,

$$\delta u_0 : \frac{\partial N_{xx}}{\partial x} + \frac{\partial N_{xy}}{\partial y} = I_0\frac{\partial^2 u_0}{\partial t^2} - I_1\frac{\partial^2}{\partial t^2}\left(\frac{\partial w_0}{\partial x}\right) \tag{6}$$

$$\delta v_0 : \frac{\partial N_{xy}}{\partial x} + \frac{\partial N_{yy}}{\partial y} = I_0\frac{\partial^2 v_0}{\partial t^2} - I_1\frac{\partial^2}{\partial t^2}\left(\frac{\partial w_0}{\partial y}\right) \tag{7}$$

$$\delta w_0 : \frac{\partial^2 M_{xx}}{\partial x^2} + 2\frac{\partial^2 M_{xy}}{\partial x \partial y} + \frac{\partial^2 M_{yy}}{\partial y^2} + N(w_0) + q = I_0\frac{\partial^2 w_0}{\partial t^2} - I_2\frac{\partial^2}{\partial t^2}\left(\frac{\partial^2 w_0}{\partial x^2} + \frac{\partial^2 w_0}{\partial y^2}\right) + I_2\frac{\partial^2}{\partial t^2}\left(\frac{\partial u_0}{\partial x} + \frac{\partial v_0}{\partial y}\right) \tag{8}$$

$$N(w_0) = \frac{\partial}{\partial x}\left(N_{xx}\frac{\partial w_0}{\partial x} + N_{xy}\frac{\partial w_0}{\partial y}\right) + \frac{\partial}{\partial y}\left(N_{xy}\frac{\partial w_0}{\partial x} + N_{yy}\frac{\partial w_0}{\partial y}\right) \tag{9}$$

where, the quantities N_{ij} are called the in-plane force resultants and M_{ij} are called the moment resultants and (I_0, I_1, I_2) are the mass moments of inertia.

2.1.3 Navier solution methodology

The displacement fields are assumed by the following form:

$$u_0(x,y,t) = \sum_{n=1}^{\infty}\sum_{m=1}^{\infty} U_{mn}(t)\cos\alpha x \sin\beta y \tag{10}$$

$$v_0(x,y,t) = \sum_{n=1}^{\infty}\sum_{m=1}^{\infty} V_{mn}(t)\sin\alpha x \cos\beta y \tag{11}$$

$$w_0(x,y,t) = \sum_{n=1}^{\infty}\sum_{m=1}^{\infty} W_{mn}(t)\sin\alpha x \sin\beta y \tag{12}$$

where U_{mn}, V_{mn} and W_{mn} are the coefficients that should be determined and $\alpha = m\pi/a$ and $\beta = n\pi/b$.

The consideration of Eqs. (10) – (12), shows that the mechanical transverse load q should also be expanded in a double sine series. Thus,

$$q(x,y,t) = \sum_{n=1}^{\infty}\sum_{m=1}^{\infty} Q_{mn}(t)\sin\alpha x \sin\beta y \tag{13}$$

$$Q_{mn}(t) = \frac{4}{ab}\int_0^a\int_0^b q(x,y,t)\sin\alpha x \sin\beta y \; dx\, dy \tag{14}$$

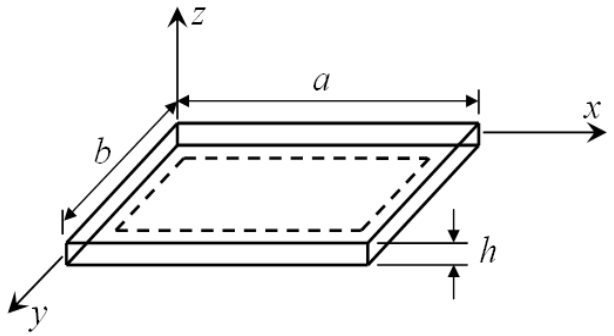

Figure 1. The geometry of simply supported rectangular laminated plates used in the analytical solutions.

Substituting expansions (10–12) into expressions given in Eqs. (6-8) without thermal loads yields

$$\begin{aligned}
&\sum_{n=1}^{\infty}\sum_{m=1}^{\infty}\big[-(A_{11}\alpha^2+A_{66}\beta^2)U_{mn}(t)\\
&\quad-(A_{12}+A_{66})\alpha\beta V_{mn}(t)\\
&\quad+\big(B_{11}\alpha^3+\tilde{B}_{12}\alpha\beta^2\big)W_{mn}(t)\\
&\quad-I_0\ddot{U}_{mn}\\
&\quad+I_1\alpha\ddot{W}_{mn}\big]\cos\alpha x\sin\beta y=0\\
&\sum_{n=1}^{\infty}\sum_{m=1}^{\infty}\big[-(A_{12}+A_{66})\alpha\beta U_{mn}(t)\\
&\quad-(A_{66}\alpha^2+A_{22}\beta^2)V_{mn}(t)\\
&\quad+\big(B_{22}\beta^3+\tilde{B}_{12}\beta\alpha^2\big)W_{mn}(t)\\
&\quad-I_0\ddot{V}_{mn}\\
&\quad+I_1\beta\ddot{W}_{mn}\big]\sin\alpha x\sin\beta y=0\\
&\sum_{n=1}^{\infty}\sum_{m=1}^{\infty}\big[\big(B_{11}\alpha^3+\tilde{B}_{12}\alpha\beta^2\big)U_{mn}(t)\\
&\quad+\big(\tilde{B}_{12}\beta\alpha^2+B_{22}\beta^3\big)V_{mn}(t)\\
&\quad-\big(D_{11}\alpha^4+2\widetilde{D}_{12}\alpha^2\beta^2\\
&\quad+D_{22}\beta^4\big)W_{mn}(t)\\
&\quad-\big(\hat{N}_{xx}\alpha^2+\hat{N}_{yy}\beta^2\big)W_{mn}(t)\\
&\quad+I_1\alpha\ddot{U}_{mn}+I_1\beta\ddot{V}_{mn}-(I_0\\
&\quad+I_2(\alpha^2\\
&\quad+\beta^2)\ddot{W}_{mn}\big]\sin\alpha x\sin\beta y\\
&\quad=-q(x,y)
\end{aligned}\tag{15}$$

where A_{ij}, D_{ij} and B_{ij} are called extensional, bending and bending-extensional coupling stiffness, respectively [23]. Also, $\hat{B}_{12}=B_{12}+2B_{66}$ and $\widehat{D}_{12}=D_{12}+2D_{66}$. Note that the edge shear force is necessarily zero.

Substituting the expansion (13) into (15), we obtain expressions of the form

$$\begin{aligned}
&\sum_{n=1}^{\infty}\sum_{m=1}^{\infty}a_{mn}(t)\cos\alpha x\sin\beta y=0\\
&\sum_{n=1}^{\infty}\sum_{m=1}^{\infty}b_{mn}(t)\sin\alpha x\cos\beta y=0\\
&\sum_{n=1}^{\infty}\sum_{m=1}^{\infty}c_{mn}(t)\sin\alpha x\sin\beta y=0
\end{aligned}\tag{16}$$

where a_{mn}, b_{mn} and c_{mn} are coefficients whose explicit form will be given shortly. Since Eq. (16) must hold for any m, n, x and y, it follows that a_{mn}=0, b_{mn}=0 and c_{mn}=0 for every m and n. The explicit forms of these coefficients are given by:

$$\begin{aligned}
a_{mn}\equiv&-(A_{11}\alpha^2+A_{66}\beta^2)U_{mn}\\
&-(A_{12}+A_{66})\alpha\beta V_{mn}\\
&+\big(B_{11}\alpha^3+\tilde{B}_{12}\alpha\beta^2\big)W_{mn}\\
&-I_0\ddot{U}_{mn}+I_1\alpha\ddot{W}_{mn}=0\\
b_{mn}\equiv&-(A_{12}+A_{66})\alpha\beta U_{mn}\\
&-(A_{66}\alpha^2+A_{22}\beta^2)V_{mn}\\
&+\big(B_{22}\beta^3+\tilde{B}_{12}\beta\alpha^2\big)W_{mn}\\
&-I_0\ddot{V}_{mn}+I_1\beta\ddot{W}_{mn}=0
\end{aligned}\tag{17}$$

$$\begin{aligned}
c_{mn}\equiv&\big[\big(B_{11}\alpha^3+\tilde{B}_{12}\alpha\beta^2\big)U_{mn}\\
&+\big(\tilde{B}_{12}\beta\alpha^2+B_{22}\beta^3\big)V_{mn}\\
&-\big(D_{11}\alpha^4+2\widetilde{D}_{12}\alpha^2\beta^2\\
&+D_{22}\beta^4\big)W_{mn}+Q_{mn}+I_1\alpha\ddot{U}_{mn}\\
&+I_1\beta\ddot{V}_{mn}-(I_0\\
&+I_2(\alpha^2+\beta^2))\ddot{W}_{mn}\big]=0
\end{aligned}$$

or in matrix form

$$\begin{aligned}
&\begin{bmatrix}\hat{c}_{11}&\hat{c}_{12}&\hat{c}_{13}\\ \hat{c}_{12}&\hat{c}_{22}&\hat{c}_{23}\\ \hat{c}_{13}&\hat{c}_{23}&\hat{c}_{33}+\tilde{s}_{33}\end{bmatrix}\begin{Bmatrix}U_{mn}\\V_{mn}\\W_{mn}\end{Bmatrix}\\
&\quad+\begin{bmatrix}\hat{m}_{11}&0&-I_1\alpha\\0&\hat{m}_{22}&-I_1\beta\\-I_1\alpha&-I_1\beta&\hat{m}_{33}\end{bmatrix}\begin{Bmatrix}\ddot{U}_{mn}\\\ddot{V}_{mn}\\\ddot{W}_{mn}\end{Bmatrix}\\
&\quad=\begin{Bmatrix}0\\0\\Q_{mn}\end{Bmatrix}
\end{aligned}\tag{18}$$

where $\hat{c}_{ij}$ is

$$\begin{aligned}
&\hat{C}_{11}=(A_{11}\alpha^2+A_{66}\beta^2)\\
&\hat{C}_{12}=(A_{12}+A_{66})\alpha\beta\\
&\hat{C}_{13}=-B_{11}\alpha^3-(B_{12}+2B_{66})\alpha\beta^2\\
&\hat{C}_{22}=(A_{66}\alpha^2+A_{22}\beta^2)\\
&\hat{C}_{23}=-B_{22}\beta^3-(B_{12}+2B_{66})\beta\alpha^2\\
&\hat{C}_{33}=D_{22}\beta^4+2(D_{12}+2D_{66})\beta^2\alpha^2+D_{11}\alpha^4\\
&\tilde{s}_{33}=\alpha^2\hat{N}_{xx}+\beta^2\hat{N}_{yy}\\
&\hat{m}_{11}=\hat{m}_{22}=I_0\\
&\hat{m}_{33}=(I_0+I_2(\alpha^2+\beta^2))
\end{aligned}\tag{19}$$

Eqs. (18) provide three second-order differential equations among the three variables U_{mn}, V_{mn} and W_{mn} for any fixed values of m and n.

For free vibration, all applied loads and the in-plane forces are set to zero, and we assume a periodic solution of the form:

$$\begin{aligned}
&U_{mn}(t)=U_{mn}^0e^{i\omega t},\\
&V_{mn}(t)=V_{mn}^0e^{i\omega t},W_{mn}(t)=W_{mn}^0e^{i\omega t}
\end{aligned}\tag{20}$$

where i = $\sqrt{-1}$ and ω is the frequency of natural vibration. Then Eq. (18) reduces to the eigenvalue problem:

$$\Big(\begin{bmatrix}\hat{c}_{11}&\hat{c}_{12}&\hat{c}_{13}\\ \hat{c}_{12}&\hat{c}_{22}&\hat{c}_{23}\\ \hat{c}_{13}&\hat{c}_{23}&\hat{c}_{33}\end{bmatrix}-\omega^2\begin{bmatrix}\hat{m}_{11}&0&0\\0&\hat{m}_{22}&0\\0&0&\hat{m}_{33}\end{bmatrix}\Big)\begin{Bmatrix}U_{mn}^0\\V_{mn}^0\\W_{mn}^0\end{Bmatrix}=\begin{Bmatrix}0\\0\\0\end{Bmatrix}\tag{21}$$

For a nontrivial solution, the determinant of the coefficient matrix in (21) should be zero, which yields the characteristic polynomial

$$-p\lambda^3+q\lambda^2-r\lambda+s=0\,,\tag{22}$$

where $\lambda=\omega^2$ is the eigenvalue and

$$p=\begin{bmatrix}\hat{m}_{11}&0&0\\0&\hat{m}_{22}&0\\0&0&\hat{m}_{33}\end{bmatrix},s=\begin{bmatrix}\hat{c}_{11}&\hat{c}_{12}&\hat{c}_{13}\\ \hat{c}_{12}&\hat{c}_{22}&\hat{c}_{23}\\ \hat{c}_{13}&\hat{c}_{23}&\hat{c}_{33}\end{bmatrix}\tag{23}$$

$$q=\begin{bmatrix}\hat{c}_{11} & 0 & 0\\ \hat{c}_{12} & \hat{m}_{22} & 0\\ \hat{c}_{13} & 0 & \hat{m}_{33}\end{bmatrix}+\begin{bmatrix}\hat{m}_{11} & \hat{c}_{12} & 0\\ 0 & \hat{c}_{22} & 0\\ 0 & \hat{c}_{23} & \hat{m}_{33}\end{bmatrix}+\begin{bmatrix}\hat{m}_{11} & 0 & \hat{c}_{13}\\ 0 & \hat{m}_{22} & \hat{c}_{23}\\ 0 & 0 & \hat{c}_{33}\end{bmatrix}$$

$$r=\begin{bmatrix}\hat{c}_{11} & \hat{c}_{12} & 0\\ \hat{c}_{12} & \hat{c}_{22} & 0\\ \hat{c}_{13} & \hat{c}_{23} & \hat{m}_{33}\end{bmatrix}+\begin{bmatrix}\hat{c}_{11} & 0 & \hat{c}_{13}\\ \hat{c}_{12} & \hat{m}_{22} & \hat{c}_{23}\\ \hat{c}_{13} & 0 & \hat{c}_{33}\end{bmatrix}+\begin{bmatrix}\hat{m}_{11} & \hat{c}_{12} & \hat{c}_{13}\\ 0 & \hat{c}_{22} & \hat{c}_{23}\\ 0 & \hat{c}_{23} & \hat{c}_{33}\end{bmatrix}$$

The real positive roots of this cubic equation give the square of the natural frequency ω_{mn} associated with mode (*m,n*). The smallest of the frequencies is called the fundamental frequency. In general, ω_{11} is not the fundamental frequency; the smallest frequency might occur for values other than $m = n = 1$.

If the in-plane inertias are neglected (i.e., $\hat{m}_{11} = \hat{m}_{22} = 0$), and irrespective of whether the rotary inertia is zero, Eq. (22) will be

$$\omega^2=\frac{1}{\hat{m}_{33}}\left(\hat{c}_{33}-\frac{\hat{c}_{13}\hat{c}_{22}-\hat{c}_{23}\hat{c}_{12}}{\hat{c}_{11}\hat{c}_{22}-\hat{c}_{12}\hat{c}_{12}}\hat{c}_{13}-\frac{\hat{c}_{11}\hat{c}_{23}-\hat{c}_{12}\hat{c}_{13}}{\hat{c}_{11}\hat{c}_{22}-\hat{c}_{12}\hat{c}_{12}}\hat{c}_{23}\right) \quad (24)$$

Note that if the in-plane inertias are not neglected, the eigenvalue problem cannot be simplified to a single equation, even if the rotary inertia is zero.

2.2. First-order shear deformation theory (FSDT)

2.2.1 Displacement and strains

Under the same assumptions and restrictions as in the classical laminate theory, the displacement field of the first-order theory is of the form:

$$\begin{aligned}u(x,y,z,t)&=u_0(x,y,t)+z\phi_x(x,y,t)\\ v(x,y,z,t)&=v_0(x,y,t)+z\phi_y(x,y,t)\\ w(x,y,z,t)&=w_0(x,y,t)\end{aligned} \quad (25)$$

Where

$$\phi_x=\frac{\partial u}{\partial z},\phi_y=\frac{\partial v}{\partial z} \quad (26)$$

which indicate that ϕ_x and ϕ_y are the rotations of a transverse normal about the *y*- and *x*- axes, respectively. The nonlinear strains associated with the displacement field (25) are obtained as

$$\begin{aligned}\varepsilon_{xx}&=\frac{\partial u_0}{\partial x}+\frac{1}{2}\left(\frac{\partial w_0}{\partial x}\right)^2+z\frac{\partial \phi_x}{\partial x}\\ \varepsilon_{yy}&=\frac{\partial v_0}{\partial y}+\frac{1}{2}\left(\frac{\partial w_0}{\partial y}\right)^2+z\frac{\partial \phi_y}{\partial y}\\ \gamma_{xy}&=\left(\frac{\partial u_0}{\partial y}+\frac{\partial v_0}{\partial x}+\frac{\partial w_0}{\partial x}\frac{\partial w_0}{\partial y}\right)+z\left(\frac{\partial \phi_x}{\partial y}+\frac{\partial \phi_y}{\partial x}\right)\\ \gamma_{xz}&=\frac{\partial w_0}{\partial x}+\phi_x,\gamma_{yz}=\frac{\partial w_0}{\partial y}+\phi_y,\varepsilon_{zz}=0\end{aligned} \quad (27)$$

Note that the strains $(\varepsilon_{xx},\varepsilon_{yy},\gamma_{xy})$ are linear through the laminate thickness, whereas the transverse shear strains $(\gamma_{xz},\gamma_{yz})$ are constant through the thickness of the laminate in the first-order laminated theory. These strains have the fo

$$\begin{Bmatrix}\varepsilon_{xx}\\ \varepsilon_{yy}\\ \gamma_{yz}\\ \gamma_{xz}\\ \gamma_{xy}\end{Bmatrix}=\begin{Bmatrix}\varepsilon^0_{xx}\\ \varepsilon^0_{yy}\\ \gamma^0_{yz}\\ \gamma^0_{xz}\\ \gamma^0_{xy}\end{Bmatrix}+z\begin{Bmatrix}\varepsilon^1_{xx}\\ \varepsilon^1_{yy}\\ \gamma^1_{yz}\\ \gamma^1_{xz}\\ \gamma^1_{xy}\end{Bmatrix} \quad (28)$$

2.2.2 Equilibrium equations

The governing equations of the first-order theory will be derived using the dynamic version of the principle of virtual displacements. The Euler-Lagrange equations are obtained as follows

$$\begin{aligned}\delta u_0&:\frac{\partial N_{xx}}{\partial x}+\frac{\partial N_{xy}}{\partial y}=I_0\frac{\partial^2 u_0}{\partial t^2}+I_1\frac{\partial^2 \phi_x}{\partial t^2}\\ \delta v_0&:\frac{\partial N_{xy}}{\partial x}+\frac{\partial N_{yy}}{\partial y}=I_0\frac{\partial^2 v_0}{\partial t^2}+I_1\frac{\partial^2 \phi_y}{\partial t^2}\\ \delta w_0&:\frac{\partial Q_x}{\partial x}+\frac{\partial Q_y}{\partial y}+N(w_0)+q=I_0\frac{\partial^2 v_0}{\partial t^2}\\ \delta \phi_x&:\frac{\partial M_{xx}}{\partial x}+\frac{\partial M_{xy}}{\partial y}-Q_x=I_2\frac{\partial^2 \phi_x}{\partial t^2}+I_1\frac{\partial^2 u_0}{\partial t^2}\\ \delta \phi_y&:\frac{\partial M_{xy}}{\partial x}+\frac{\partial M_{yy}}{\partial y}-Q_y=I_2\frac{\partial^2 \phi_y}{\partial t^2}+I_1\frac{\partial^2 v_0}{\partial t^2},\end{aligned} \quad (29)$$

where Q_x and Q_y are called transverse force resultants and

$$\begin{Bmatrix}Q_x\\ Q_y\end{Bmatrix}=K\int_{-h/2}^{h/2}\begin{Bmatrix}\sigma_{xz}\\ \sigma_{yz}\end{Bmatrix}dz \quad (30)$$

Parameter K is called a shear correction coefficient and is used because of a discrepancy between the actual stress state and the constant stress state predicted by the first-order theory.

2.2.2 Boundary condition

The natural boundary conditions are obtained by setting the coefficients of $\delta u_n, \delta u_s, \delta w_0, \delta \phi_n$ and $\delta \phi_s$ to zero separately:

$$N_{nn} - \widehat{N}_{nn} = 0, N_{ns} - \widehat{N}_{ns} = 0, Q_n - \widehat{Q}_n = 0, M_{nn} - \widehat{M}_{nn} = 0, M_{ns} - \widehat{M}_{ns} = 0 \quad (31)$$

where

$$Q_n \equiv Q_x n_x + Q_y n_y + P(w_0) \quad (32)$$

Thus, the primary and secondary variables of the theory are

primary variables: $u_n, u_s, w_0, \phi_n, \phi_s$
secondary variables :$N_{nn}, N_{ns}, Q_n, M_{nn}, M_{ns}$ (33)

The initial conditions of the theory involve specifying the values of the displacements and their first derivatives with respect to time at $t = 0$.

2.2.3 Equations of motion

The boundary conditions are satisfied by the following expansions

$$u_0(x,y,t) = \sum_{n=1}^{\infty}\sum_{m=1}^{\infty} U_{mn}(t)\cos\alpha x \sin\beta y$$
$$v_0(x,y,t) = \sum_{n=1}^{\infty}\sum_{m=1}^{\infty} V_{mn}(t)\sin\alpha x \cos\beta y$$
$$w_0(x,y,t) = \sum_{n=1}^{\infty}\sum_{m=1}^{\infty} W_{mn}(t)\sin\alpha x \sin\beta y \quad (34)$$
$$\phi_x(x,y,t) = \sum_{n=1}^{\infty}\sum_{m=1}^{\infty} X_{mn}(t)\cos\alpha x \sin\beta y$$
$$\phi_y(x,y,t) = \sum_{n=1}^{\infty}\sum_{m=1}^{\infty} Y_{mn}(t)\sin\alpha x \cos\beta y$$

The Navier solution can be calculated from

$$\begin{bmatrix} \hat{s}_{11} & \hat{s}_{12} & 0 & \hat{s}_{14} & \hat{s}_{15} \\ \hat{s}_{12} & \hat{s}_{22} & 0 & \hat{s}_{24} & \hat{s}_{25} \\ 0 & 0 & \hat{s}_{33}+\tilde{s}_{33} & \hat{s}_{34} & \hat{s}_{35} \\ \hat{s}_{14} & \hat{s}_{24} & \hat{s}_{34} & \hat{s}_{44} & \hat{s}_{45} \\ \hat{s}_{15} & \hat{s}_{25} & \hat{s}_{35} & \hat{s}_{45} & \hat{s}_{55} \end{bmatrix} \begin{Bmatrix} U_{mn} \\ V_{mn} \\ W_{mn} \\ X_{mn} \\ Y_{mn} \end{Bmatrix} + \begin{bmatrix} \widehat{m}_{11} & \hat{s}_{12} & 0 & \hat{s}_{14} & \hat{s}_{15} \\ \hat{s}_{12} & \widehat{m}_{22} & 0 & \hat{s}_{24} & \hat{s}_{25} \\ 0 & 0 & \widehat{m}_{33} & \hat{s}_{34} & \hat{s}_{35} \\ \hat{s}_{14} & \hat{s}_{24} & \hat{s}_{34} & \widehat{m}_{44} & \hat{s}_{45} \\ \hat{s}_{15} & \hat{s}_{25} & \hat{s}_{35} & \hat{s}_{45} & \widehat{m}_{55} \end{bmatrix} \begin{Bmatrix} \ddot{U}_{mn} \\ \ddot{V}_{mn} \\ \ddot{W}_{mn} \\ \ddot{X}_{mn} \\ \ddot{Y}_{mn} \end{Bmatrix} = \begin{Bmatrix} 0 \\ 0 \\ Q_{mn} \\ 0 \\ 0 \end{Bmatrix} - \begin{Bmatrix} U_{mn} \\ V_{mn} \\ W_{mn} \\ X_{mn} \\ Y_{mn} \end{Bmatrix} \begin{Bmatrix} \alpha N^1_{mn} \\ \beta N^2_{mn} \\ 0 \\ \alpha M^1_{mn} \\ \beta M^2_{mn} \end{Bmatrix} \quad (35)$$

where

$$\hat{s}_{11} = (A_{11}\alpha^2 + A_{66}\beta^2), \hat{s}_{12} = (A_{12} + A_{66})\alpha\beta$$
$$\hat{s}_{14} = (B_{11}\alpha^2 + B_{66}\beta^2), \hat{s}_{15} = (B_{12} + B_{66})\alpha\beta$$
$$\hat{s}_{22} = (A_{66}\alpha^2 + A_{22}\beta^2), \hat{s}_{24} = \hat{s}_{15} \quad (36)$$
$$\hat{s}_{25} = (B_{66}\alpha^2 + B_{22}\beta^2), \hat{s}_{34} = KA_{55}\alpha$$
$$\hat{s}_{33} = K(A_{55}\alpha^2 + A_{44}\beta^2), \hat{s}_{35} = KA_{44}\beta$$
$$\tilde{s}_{33} = \widehat{N}_{xx}\alpha^2 + \widehat{N}_{yy}\beta^2, \widehat{m}_{11} = I_0, \widehat{m}_{55} = I_2$$
$$\hat{s}_{44} = D_{11}\alpha^2 + D_{66}\beta^2 + KA_{55}, \widehat{m}_{22} = I_0$$
$$\hat{s}_{45} = (D_{12} + D_{66})\alpha\beta, \widehat{m}_{33} = I_0, \widehat{m}_{44} = I_2$$
$$\hat{s}_{55} = D_{66}\alpha^2 + D_{22}\beta^2 + KA_{44}$$

For free vibration, all thermal and mechanical loads are set to zero and substitute to Eq. (29) and obtain

$$\left([\hat{S}] - \omega^2[\widehat{M}]\right)\{\Delta\} = \{0\} \quad (37)$$

where

$$[\hat{S}] = \begin{bmatrix} \hat{s}_{11} & \hat{s}_{12} & 0 & \hat{s}_{14} & \hat{s}_{15} \\ \hat{s}_{12} & \hat{s}_{22} & 0 & \hat{s}_{24} & \hat{s}_{25} \\ 0 & 0 & \hat{s}_{33} & \hat{s}_{34} & \hat{s}_{35} \\ \hat{s}_{14} & \hat{s}_{24} & \hat{s}_{34} & \hat{s}_{44} & \hat{s}_{45} \\ \hat{s}_{15} & \hat{s}_{25} & \hat{s}_{35} & \hat{s}_{45} & \hat{s}_{55} \end{bmatrix}, \quad [\widehat{M}] = \begin{bmatrix} \widehat{m}_{11} & 0 & 0 & 0 & 0 \\ 0 & \widehat{m}_{22} & 0 & 0 & 0 \\ 0 & 0 & \widehat{m}_{33} & 0 & 0 \\ 0 & 0 & 0 & \widehat{m}_{44} & 0 \\ 0 & 0 & 0 & 0 & \widehat{m}_{55} \end{bmatrix} \quad (38)$$

and $\{\Delta\}^{\mathrm{T}} = \{U^0_{mn}\ V^0_{mn}\ W^0_{mn}\ X^0_{mn}\ Y^0_{mn}\}$. When rotary inertia is omitted, Eq. (37) can be simplified by eliminating Xmn and Ymn (i.e., using the static condensation method) as follows

$$\left(\begin{bmatrix} \bar{s}_{11} & \bar{s}_{12} & \bar{s}_{13} \\ \bar{s}_{12} & \bar{s}_{22} & \bar{s}_{23} \\ \bar{s}_{13} & \bar{s}_{23} & \bar{s}_{33} \end{bmatrix} - \omega^2 \begin{bmatrix} \widehat{m}_{11} & 0 & 0 \\ 0 & \widehat{m}_{22} & 0 \\ 0 & 0 & \widehat{m}_{33} \end{bmatrix} \right) \begin{Bmatrix} U^0_{mn} \\ V^0_{mn} \\ W^0_{mn} \end{Bmatrix} = \begin{Bmatrix} 0 \\ 0 \\ 0 \end{Bmatrix} \quad (39)$$

where

$$\bar{s}_{11} = \hat{s}_{11} - \frac{(\hat{s}_{14}\hat{s}_{55} - \hat{s}_{15}\hat{s}_{45})\hat{s}_{14}}{\bar{s}_{00}} - \frac{(\hat{s}_{15}\hat{s}_{44} - \hat{s}_{14}\hat{s}_{45})\hat{s}_{15}}{\bar{s}_{00}}$$
$$\bar{s}_{12} = \hat{s}_{12} - \frac{(\hat{s}_{24}\hat{s}_{55} - \hat{s}_{25}\hat{s}_{45})\hat{s}_{14}}{\bar{s}_{00}} - \frac{(\hat{s}_{25}\hat{s}_{44} - \hat{s}_{24}\hat{s}_{45})\hat{s}_{15}}{\bar{s}_{00}}$$
$$\bar{s}_{13} = -\frac{(\hat{s}_{34}\hat{s}_{55} - \hat{s}_{35}\hat{s}_{45})\hat{s}_{14}}{\bar{s}_{00}} - \frac{(\hat{s}_{33}\hat{s}_{44} - \hat{s}_{34}\hat{s}_{45})\hat{s}_{15}}{\bar{s}_{00}}$$
$$\bar{s}_{22} = \hat{s}_{22} - \frac{(\hat{s}_{24}\hat{s}_{55} - \hat{s}_{25}\hat{s}_{45})\hat{s}_{24}}{\bar{s}_{00}} - \frac{(\hat{s}_{25}\hat{s}_{44} - \hat{s}_{24}\hat{s}_{45})\hat{s}_{25}}{\bar{s}_{00}} \quad (40)$$
$$\bar{s}_{23} = \hat{s}_{23} - \frac{(\hat{s}_{34}\hat{s}_{55} - \hat{s}_{35}\hat{s}_{45})\hat{s}_{24}}{\bar{s}_{00}} - \frac{(\hat{s}_{35}\hat{s}_{44} - \hat{s}_{34}\hat{s}_{45})\hat{s}_{25}}{\bar{s}_{00}}$$
$$\bar{s}_{33} = \hat{s}_{33} - \frac{(\hat{s}_{34}\hat{s}_{55} - \hat{s}_{35}\hat{s}_{45})\hat{s}_{34}}{\bar{s}_{00}} - \frac{(\hat{s}_{35}\hat{s}_{44} - \hat{s}_{34}\hat{s}_{45})\hat{s}_{35}}{\bar{s}_{00}}$$
$$\bar{s}_{00} = \hat{s}_{44}\hat{s}_{55} - \hat{s}_{45}\hat{s}_{45}$$

If the in-plane and rotary inertias are omitted (i.e., $\hat{m}_{11} = \hat{m}_{22} = \hat{m}_{44} = \hat{m}_{55} = 0$), we have

$$\omega^2 = \frac{1}{\hat{m}_{33}}\left(\bar{s}_{33} - \frac{\bar{s}_{13}\bar{s}_{22} - \bar{s}_{23}\bar{s}_{12}}{\bar{s}_{11}\bar{s}_{22} - \bar{s}_{12}\bar{s}_{12}}\bar{s}_{13} - \frac{\bar{s}_{11}\bar{s}_{23} - \bar{s}_{12}\bar{s}_{13}}{\bar{s}_{11}\bar{s}_{22} - \bar{s}_{12}\bar{s}_{12}}\bar{s}_{23}\right) \quad (41)$$

3. Finite Element Method

The finite element method (FEM), known as a powerful tool for many engineering problems, has been used to compute such matters as elastic-plastic, residual and thermal stresses, and buckling and vibration analysis. Because of this, ANSYS software that is a commercial FEM program was preferred for the vibration analysis of the laminated composite plates. The Shell 99 element type was selected for the 2D modeling of solid structures in ANSYS. Initially, the plates are to get an initial estimate of the undamped natural frequencies ωn and mode shape *n*. The element type of Shell 99 may be used for layered applications of a structural shell model. The element has six degrees of freedom at each node; and translations in the nodal *x* and *y* directions and rotations about the nodal *z*-axis. This element is constituted by layers designated by numbers (LN-layer number), increasing from the bottom to the top of the laminate; the last number quantifies the existing total number of layers in the laminate (NL-total number of layers). The boundary conditions have been applied to the nodes, i.e., the dimensions in the *x* and *y* are 400 mm for 2D, and the displacements and rotations of all nodes about the *y*–*z* plane are also taken as zero. The model of the laminated plate is generated with a different number of layers (based on different side-to-thickness ratio). The boundary conditions and mesh shape are shown in Fig. 2. It is mentioned that for a free- vibration analysis, the subspace method is applied. The subspace iteration method was described in detail by Bathe [24].

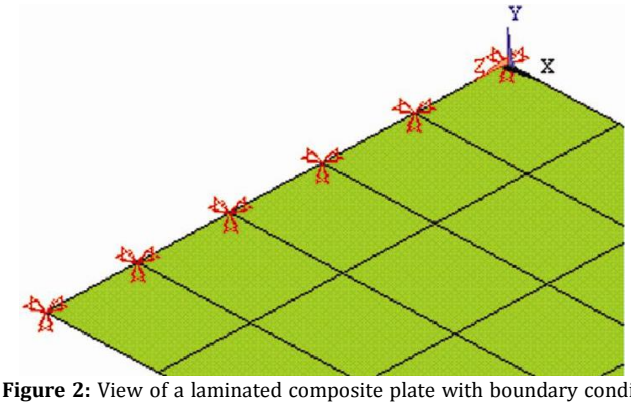

Figure 2: View of a laminated composite plate with boundary conditions and mesh shape.

After the mesh generation process, a laminated composite plate with six layers has 500 elements and 1,488 nodes. By increasing the number of layers, the numbers of elements and the nodes of the plates increase. The normal penalty stiffnesses of the contact element are chosen between 10^4 and 10^9.

4. Results and Discussions

The nondimensionalized frequencies $\overline{\omega}_{nn} = \omega_{mn}(b^2/\pi^2)\sqrt{\rho h/D_{22}}$, of specially orthotropic and antisymmetric cross-ply square laminates are presented in Table 1 for modulus ratios $E_1/E_2 = 10$ and 20 ($G_{12} = G_{13} = 0.5E_2$, $G_{23} = 0.2E_2$, $\upsilon_{12} = 0.25$). All layers are of equal thickness. Results are presented for *m,n* = 1,2,3 and for when the rotary inertia is neglected.

The fundamental frequency increases with the modular ratio. The effect of including rotary inertia is to decrease the frequency of vibration. Note that the first four frequencies for an antisymmetric cross-ply plates are (*m,n*) = (1,1), (1,2), (2,1) and (2,2) and $\omega_{mn} = \omega_{nm}$ for antisymmetric laminates. Also, good agreement was found between the analytical solution and the FEM analysis.

Fig. 3 shows a plot of fundamental frequency $\bar{\omega}$ versus aspect ratio *a/b* for symmetric $(0/90)_s$ cross-ply and antisymmetric $(0/90)_2$ cross-ply laminates. The material properties used are $E_1/E_2 = 40$, $G_{12} = G_{13} = 0.6E_2$, $G_{23} = 0.2E_2$, $\upsilon_{12} = 0.25$). Fig. 4 shows the effect of coupling between bending and extension on the fundamental frequencies of antisymmetric cross-ply laminates. The material properties used are $E_1/E_2 = 25$, $G_{12} = G_{13} = 0.5E_2$, $G_{23} = 0.2E_2$, $\upsilon_{12} = 0.25$). With an increase in the number of layers, the frequencies approach those of the orthotropic plate. The bending-stretching coupling lowers the vibration frequencies. For example, the two-layer plate has vibration frequencies about 40 percent lower than those of an eight-layer antisymmetric laminate or orthotropic plate with the same total thickness.

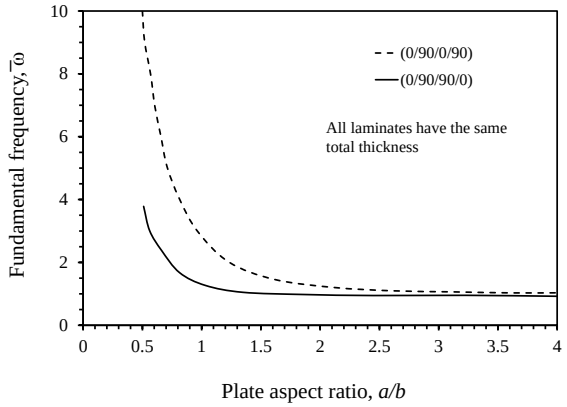

Figure 3: The nondimensionalized fundamental frequency versus the plate aspect ratio (a/b) for cross-ply laminates.

Table 1. The nondimensionalized frequencies of cross-ply laminates, according to the classical plate theory

m	n	Layup	$(0/90)$		$(0/90)_2$		$(0/90)_3$	
		Method	$\frac{E_1}{E_2}=10$	$\frac{E_1}{E_2}=20$	$\frac{E_1}{E_2}=10$	$\frac{E_1}{E_2}=20$	$\frac{E_1}{E_2}=10$	$\frac{E_1}{E_2}=20$
1	1	Analytical	1.066	0.977	1.359	1.257	1.445	1.321
		FEM	1.254	1.098	1.536	1.478	1.613	1.528
		Reddy [23]	1.183	0.990	1.479	1.386	1.545	1.469
1	2	Analytical	3.090	2.697	3.987	3.851	4.136	4.087
		FEM	3.265	2.861	4.182	4.023	4.351	4.295
		Reddy [23]	3.174	2.719	4.077	3.913	4.274	4.158
2	1	Analytical	3.090	2.697	3.987	3.851	4.136	4.087
		FEM	3.265	2.861	4.182	4.023	4.351	4.295
		Reddy [23]	3.174	2.719	4.077	3.913	4.274	4.158
2	2	Analytical	4.266	3.911	5.812	5.449	5.985	5.774
		FEM	4.882	4.078	6.081	5.631	6.227	5.937
		Reddy [23]	4.733	3.959	5.918	5.547	6.179	5.877
3	1	Analytical	6.542	5.747	8.537	8.329	8.989	8.778
		FEM	6.741	5.829	8.773	8.546	9.231	9.097
		Reddy [23]	6.666	5.789	8.698	8.456	9.136	8.998
3	2	Analytical	7.386	6.014	9.894	9.423	10.398	9.997
		FEM	8.011	6.271	10.125	9.696	10.553	10.201
		Reddy [23]	7.927	6.193	10.034	9.507	10.494	10.088

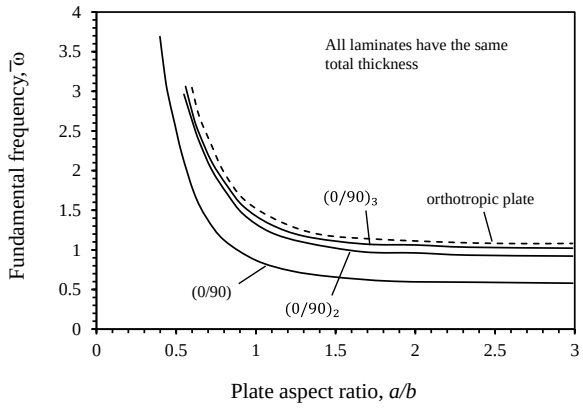

Figure 4: The nondimensionalized fundamental frequency versus the plate aspect ratio (a/b) for antisymmetric cross-ply laminates.

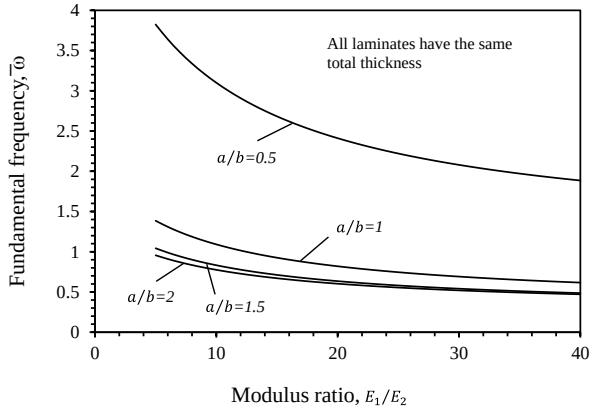

Figure 5: The nondimensionalized fundamental frequency versus the modulus ratio for antisymmetric cross-ply laminates for various plate aspect ratios.

Fig. 5 shows a plot of fundamental frequency $\bar{\omega}$ versus the modulus ratio E_1/E_2 for antisymmetric (0/90) cross-ply laminates for various values of plate aspect ratios. The plate aspect ratio lowers the vibration frequencies. The rectangle plate has vibration frequencies about 50 percent lower than those of a square plate with the same total thickness.

The nondimensionalized fundamental frequencies $\bar{\omega}_{nn} = \omega_{mn}(b^2/\pi^2)\sqrt{\rho h/D_{22}}$ of graphite-epoxy composites with $E_1/E_2 = 40$, $G_{12}/E_2 = 0.5$, $\upsilon_{12} = 0.25$ and $a/b = 1$ are shown as a function of the lamination angle in Fig. 6. The bending-stretching coupling due to the presence of B_{16} and B_{26} lowers the frequencies. The coupling is the maximum for two-layer plates, and it rapidly decreases with increasing number of layers. At $\theta = 45^{\circ}$, the fundamental fre-

quency of the two-layer plate is about 40 percent lower than that of the eight-layer laminate.

The nondimensionalized fundamental frequencies of graphite-epoxy composites with $E_1/E_2 = 40$, $G_{12}/E_2 = 0.5$, $\upsilon_{12} = 0.25$ are shown as a function of plate aspect ratios in Fig. 7. With an increase in the number of layers, the frequencies approach those of the orthotropic plate. The bending-stretching coupling lowers the vibration frequencies. For example, the two-layer plate has vibration frequencies about 40 percent lower than those of a four-layer antisymmetric angle-ply laminate or orthotropic plate with the same total thickness and aspect ratio. Also, effects of an aspect ratio on the fundamental frequencies of a laminated composite with same total thickness are more significant for values less than 1.

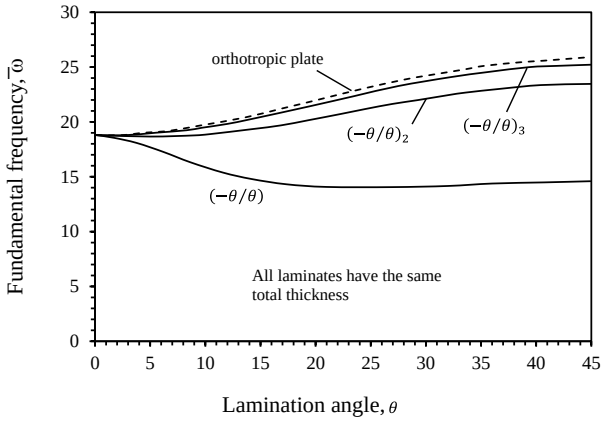

Figure 6: The nondimensionalized fundamental frequency versus the lamination angle of antisymmetric angle-ply square laminates.

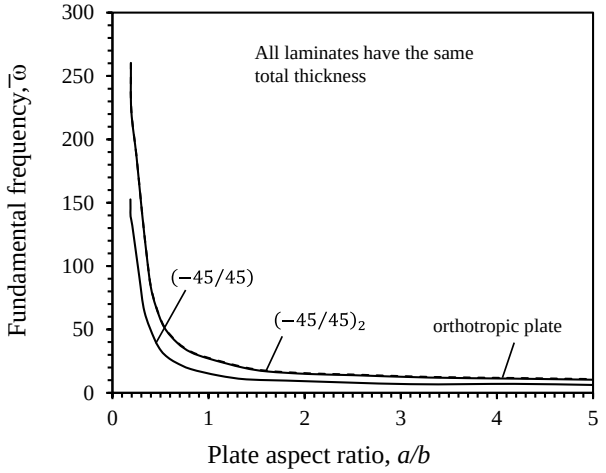

Figure 7: The nondimensionalized fundamental frequency versus the plate aspect ratio of antisymmetric angle-ply laminates.

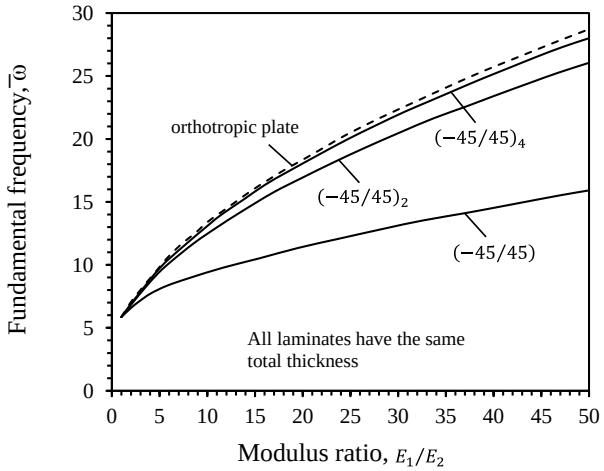

Figure 8: The nondimensionalized fundamental frequency versus the modulus ratio of antisymmetric angle-ply square laminates.

Fig. 8 shows a nondimensionalized fundamental frequency versus a modulus ratio of antisymmetric angle-ply square laminates. The effect of coupling is significant for all modulus ratios and the difference between the two-layer solution and orthotropic solution increases with the modulus ratio.

Table 2 and 3 contain the nondimensionalized fundamental frequencies $\bar{\omega}_{nn} = \omega_{mn}(a^2/h)\sqrt{\rho/E}$ for symmetric cross-ply laminates using the FSDT. The effect of the shear correction factor is to decrease the frequencies. The smaller the K, the smaller the frequencies are. The rotary inertia (RI) also decreases the frequencies.

Fig. 9 shows the effect of transverse shear deformation and rotary inertia on the fundamental natural frequencies of orthotropic and symmetric cross-ply (0/90/90/0) square plates with the following lamina properties:

$E_1/E_2 = 25$, $G_{12} = G_{13} = 0.5E_2$, $G_{23} = 0.2E_2$, $\upsilon_{12} = 0.25$.

The symmetric cross-ply plate behaves much like an orthotropic plate. The effect of rotary inertia is negligible in the FSDT and, therefore, is not shown in the figure.

Fig. 10 shows the effect of transverse shear deformation, bending-extensional coupling and rotary inertia on the fundamental natural frequencies of two-layer and eight-layer antisymmetric cross-ply laminates ($E_1/E_2 = 25$, $G_{12} = G_{13} = 0.5E_2$, $G_{23} = 0.2E_2$, $\upsilon_{12} = 0.25$).

Table 2. The effect of shear deformation on the dimensionless natural frequencies of simply supported symmetric cross-ply plates.

a/h	Theory	0°	Three-ply	Five-ply	Seven-ply	Nine-ply
	FSDT	8.388✷	8.094	8.569	8.673	8.713
		9.019	8.698	9.197	9.312	9.357
5		9.534	9.196	9.706	9.829	9.877
	FEM	9.643	9.234	9.857	9.997	10.017
	CLPT	14.750	14.750	14.750	14.750	14.750
	FSDT	12.067	11.730	12.167	12.290	12.342
		12.540	12.223	12.621	12.735	12.783
10		12.890	12.592	12.956	13.062	13.107
	FEM	12.901	12.668	13.078	13.215	13.295
	CLPT	15.104	15.104	15.104	15.104	15.104
	FSDT	14.220	14.042	14.229	14.288	14.312
		14.411	14.254	14.412	14.461	14.461
20		14.542	14.402	14.538	14.580	14.598
	FEM	14.568	14.523	14.638	14.705	14.712
	CLPT	15.197	15.197	15.197	15.197	15.197
	FSDT	14.569	14.433	14.563	14.604	14.621
		14.700	14.582	14.688	14.722	14.737
25		14.789	14.682	14.774	14.803	14.815
	FEM	14.812	14.723	14.835	14.907	14.918
	CLPT	15.208	15.208	15.208	15.208	15.208
	FSDT	15.079	15.015	15.052	15.063	15.068
		15.115	15.057	15.086	15.096	15.100
50		15.139	15.085	15.110	15.117	15.121
	FEM	15.238	15.128	15.262	15.236	15.240
	CLPT	15.223	15.223	15.223	15.223	15.223
	FSDT	15.215	15.173	15.183	15.186	15.187
		15.225	15.184	15.192	15.194	15.195
100		15.231	15.191	15.198	15.200	15.200
		15.312	15.284	15.293	15.301	15.302
	CLPT	15.227	15.227	15.227	15.227	15.227

✷The first line corresponds to the shear correction coefficient of K=2/3 and the second and third lines correspond to the shear correction coefficient of K=5/6 and K=1.0, respectively.

Table 3. The effect of shear deformation, rotary inertia and the shear correction coefficient on the dimensionless natural frequencies of simply supported symmetric cross-ply (0/90/0) plates

a/h	*m*	*n*	CLPT w/o RI	CLPT with RI	FSDT w/o RI	FSDT with RI
10	1	1	15.228	1.104	12.593	12.573✷
					12.223	12.163
	1	2	22.877	22.421	19.440	19.203
					18.942	18.729
	1	3	40.229	38.738	32.496	31.921
					31.421	30.932
	2	1	56.885	55.751	33.097	32.931
					31.131	30.991
	2	2	60.911	59.001	36.786	36.362
					34.794	34.434
	1	4	66.754	62.526	48.837	47.854
					46.714	45.923
	2	3	71.522	67.980	45.484	44.720
					43.212	42.585
100	1	1	15.228	15.227	15.192	15.191
					15.185	15.183
	1	2	22.877	22.873	22.831	22.827
					22.822	22.817
	1	3	40.299	40.283	40.190	40.147
					40.169	40.153
	2	1	56.885	56.874	56.330	56.319
					56.221	56.210
	2	2	60.911	60.891	60.342	60.322
					60.230	60.211
	1	4	66.754	66.708	66.466	66.421
					66.409	66.364
	2	3	71.522	71.484	70.919	70.882
					70.801	70.764

✷The first line corresponds to the shear correction coefficient of K=1.0 and the second line corresponds to the shear correction coefficient of K=5/6.

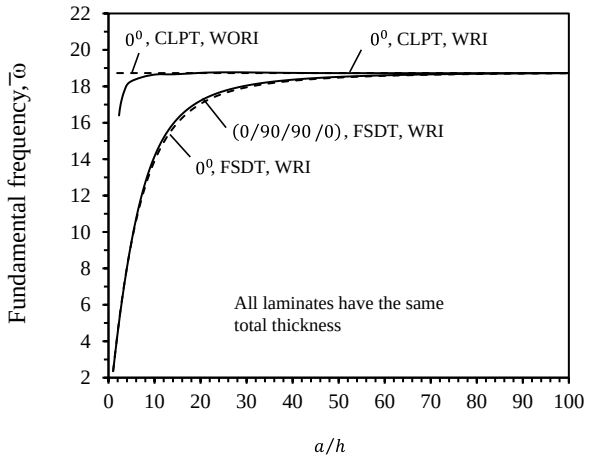

Figure 9: The nondimensionalized fundamental frequency versus the side-to-thickness ratio for simply supported orthotropic and symmetric cross-ply (0/90/90/0) laminates.

. The eight-layer antisymmetric cross-ply plate behaves much like an orthotropic plate. The effect of rotary inertia is negligible in the FSDT and, therefore, is not shown in the figure.

Table 4 contains numerical values of the fundamental frequencies of antisymmetric cross-ply laminated plates for various modular ratios. The results for both two-layer and eight-layer laminated plates for square and rectangular geometries are presented.

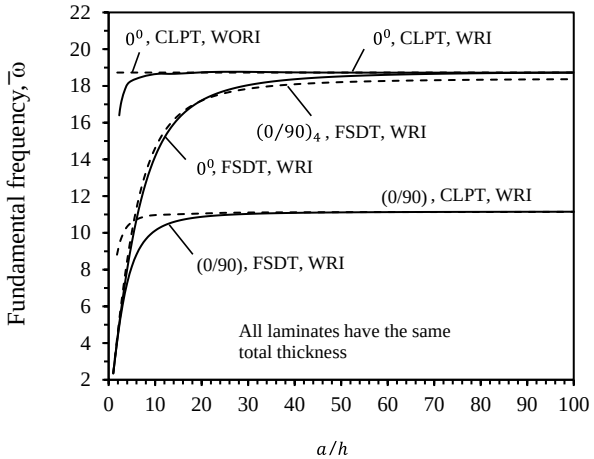

Figure 10: The nondimensionalized fundamental frequency versus the side-to-thickness ratio for simply supported orthotropic and antisymmetric cross-ply (0/90) laminates.

Table 4. The effect of shear deformation on the nondimensionalized fundamental frequencies of simply supported antisymmetric cross-ply plates.

		$E_1/E_2 = 10$		$E_1/E_2 = 25$		$E_1/E_2 = 40$	
b/h	Theory	$(0/90)$	$(0/90)_4$	$(0/90)$	$(0/90)_4$	$(0/90)$	$(0/90)_4$
Square plate (a/b=1)							
10	FSDT	7.530	9.507	8.990	12.683	10.122	14.611
	CLPT	7.832	10.268	9.566	14.816	11.011	18.265
100	FSDT	7.927	10.345	9.688	14.913	11.152	18.366
	CLPT	7.931	10.354	9.695	14.941	11.163	18.419
Rectangular plate (a/b=3)							
10	FSDT	4.780	6.341	5.988	8.824	6.884	10.290
	CLPT	4.930	6.772	6.324	10.201	7.437	12.738
100	FSDT	4.962	6.798	6.367	10.231	7.487	12.763
	CLPT	4.964	6.804	6.372	10.249	7.493	12.798
Rectangular plate (a/b=5)							
10	FSDT	4.631	6.209	5.863	8.707	6.769	10.170
	CLPT	4.825	6.612	6.332	10.200	7.582	12.729
100	FSDT	4.806	6.657	6.236	10.108	7.364	12.640
	CLPT	4.809	6.667	6.243	10.117	7.371	12.643

5. Conclusions

Analytical and numerical solutions for the free vibration of laminated polymeric composite plates with different layups are compaired based on different plate theories. Also, the effects of some parameters on the fundamental frequencies of laminated plate were performed. As a verification method, an FEM was applied with ANSYS to compare the results with those obtained from a closed-form solution. Based on the results observed, the following comments are as such:

- The fundamental frequency increases with the modular ratio. The effect of including rotary inertia is to decrease the frequency of vibration.
- The bending-stretching coupling lowers the vibration frequencies.
- The plate aspect ratio lowers the vibration frequencies. The rectangle plate has vibration frequencies about 50 percent lower than those of a square plate with the same total thickness.
- The effect of the shear correction factor is to decrease the frequencies. The smaller the K, the smaller the frequencies. The rotary inertia (RI) also decreases frequencies.
- In all cases, results obtained from the FEM are in good agreement with analytical outputs. Also, it is shown that the FEM predicted higher values, which is reported in the literature review presented [14, 18-19].
- The finite element model presented has an acceptable accuracy for utilizing this model for the analysis of more complicated cases.

References

[1] Campbell FC. **Structural composite materials**, ASM international; 2011.

[2] Tan p, Nie JG. Free and forced vibration of variable stiffness composite annular thin plates with elastically restrained edges. *Compos Struct* 2016; 149: 398-407.

[3] Zhang LW, Zhang Y, Zou GL, Liew KM. Free vibration analysis of triangular CNT-reinforced composite plates subjected to in-plane stresses using FSDT element-free method. *Compos Struct* 2016*;* 149: 247-260.

[4] Chakraborty S, Mandal B, Chowdhury R, Chakrabarti A. Stochastic free vibration analysis of laminated composite plates using polynomial correlated function expansion. *Compos Struct* 2016; 135: 236-249.

[5] Ganesh S, Kumar KS, Mahato PK. Free Vibration Analysis of Delaminated Composite Plates Using Finite Element Method. *Int Conf Vib Problems*; 2015. 1067-1075.

[6] Mantari JL, Ore M. Free vibration of single and sandwich laminated composite plates by using a simplified FSDT. *Compos Struct* 2015; 132: 952-959.

[7] Su Z, Jin G, Wang X. Free vibration analysis of laminated composite and functionally graded sector plates with general boundary conditions. *Compos Struct* 2015*;* 132: 720-736.

[8] Zhang LW, Lei ZX, Liew KM. Free vibration analysis of functionally graded carbon nanotube-reinforced composite triangular plates using the FSDT and element-free IMLS-Ritz method. *Compos Struct* 2015; 120: 189-199.

[9] Marjanivic M, Vuksanovic D. Layerwise solution of free vibrations and buckling of laminated composite and sandwich plates with embedded delamination. *Compos Struct* 2014*;* 108: 9-20.

[10] Boscolo M. Analytical solution for free vibration analysis of composite plates with layerwise displacement assumptions. *Compos Struct* 2013; 100: 493-510.

[11] Qu Y, Wu S, Li H, Meng G. Three-dimensional free and transient vibration analysis of composite laminated and sandwich rectangular parallelepipeds: Beams, plates and solids. *Compos Part B: Eng* 2015; 73: 96-110.

[12] Rafiee M, Liu XF, He XQ, Kitipornchai S. Geometrically nonlinear free vibration of shear deformable piezoelectric carbon nanotube/fiber/polymer multiscale laminated composite plates. *J Sound Vib* 2014; 333 (14): 3236-3251.

[13] Akhras G, Li W. Stability and free vibration analysis of thick piezoelectric composite plates using spline finite strip method. *Int J Mech Sci* 2011; 53 (8): 575-584.

[14] Grover N, Singh BN, Maiti DK. Analytical and finite element modeling of laminated composite and sandwich plates: An assessment of a new shear deformation theory for free vibration response. *Int J Mech Sci* 2013; 67: 89-99.

[15] Jafari RA, Abedi M, Kargarnovin MH, Ahmadian MT. An analytical approach for the free vibration analysis of generally laminated composite beams with shear effect and rotary inertia. *Int J Mech Sci* 2012; 65 (1): 97-104.

[16] Tai H, Kim S. Free vibration of laminated composite plates using two variable refined plate theories. *Int J Mech Sci* 2010; 52 (4): 626-633.

[17] Srinivasa CV, Suresh JY, kumar WP. Experimental and finite element studies on free vibration of skew plates. *Int J Adv Struct Eng* 2014; 48 (6): 123-129.

[18] Ramu I, Mohanty SC. Study on Free Vibration Analysis of Rectangular Plate Structures Using Finite Element Method. *Proc Eng* 2012; 38: 2758-2766.
[19] Chandrashekhara K. Free vibration of composite beams including rotary inertia and shear deformation. *Compos Struct* 1990; 14 (4): 269-279.
[20] Ke L, Yang J, Kitipornchai S. Nonlinear free vibration of functionally graded carbon nanotube-reinforced composite beams. *Compos Struct* 2010; 92 (3): 676-683.
[21] Song O. Free Vibration of Anisotropic Composite Thin-Walled Beams of Closed Cross-Section Contour. *J Sound Vib* 1993; 167 (1): 129-147.
[22] Lee J. Free vibration analysis of delaminated composite beams. *Comput Struct* 2000; 74 (2): 121-129.
[23] Reddy JN. **Mechanics of laminated composite plates and shells, theory and analysis**. 2nd ed. CRC Press; 2003.
[24] Bathe KJ. **Finite element procedures**. Prentie-Hall, Englewood cliffs; 1996.